Effects of soft and hard magnetic particles on the mechanical performance of ultra-soft magnetorheological elastomers

M.A. Moreno-Mateos[a], M. Lopez-Donaire[a], M. Hossain[b], D. Garcia-Gonzalez[a,*]

[a]*Department of Continuum Mechanics and Structural Analysis, Universidad Carlos III de Madrid, Avda. de la Universidad 30, 28911 Leganés, Madrid, Spain*

[b]*Zienkiewicz Centre for Computational Engineering, College of Engineering, Swansea University, SA1 8EN, United Kingdom*

Abstract

Magnetorheological elastomers (MREs) mechanically respond to external magnetic stimuli by changing their mechanical properties and/or changing their shape. Recent studies have shown the great potential of MREs when manufactured with an extremely soft matrix and soft-magnetic particles. Under the application of an external magnetic field, such MREs present significant mechanical stiffening, and when the magnetic field is off, they show a softer response, being these alternative states fully reversible. Although soft-magnetic particles are suitable for their high magnetic susceptibility, they require the magnetic actuation to remain constant in order to achieve the magneto-mechanical stiffening. Here, we present an alternative solution based on hard-magnetic MREs to provide stiffening responses that can be sustained along time without the need of keeping the external magnetic field on. To this end, we manufacture novel extremely soft hard-magnetic MREs (stiffness in the order of 1 kPa) and characterise them under magneto-mechanical shear and confined magnetic expansion deformation modes, providing a comparison framework with the soft-magnetic counterparts. The extremely soft nature of the matrix allows for easily activating the magneto-mechanical couplings under external magnetic actuation. In this regard, we provide a novel approach by setting the magnetic actuation below the fully magnetic saturating field. In addition, free deformation tests provide hints on the microstructural transmission of torques from the hard-magnetic particles to the viscoelastic carrier matrix, resulting in macroscopic geometrical effects and complex functional morphological changes.

Keywords: Magnetorheological elastomers (MREs), Magneto-mechanics, Experimental characterisation, Hard-magnetics MRE, Multifunctional materials, Magnetic properties

*Corresponding authors

Email addresses: migmoren@ing.uc3m.es (M.A. Moreno-Mateos), danigarc@ing.uc3m.es (D. Garcia-Gonzalez)

1. Introduction

Smart materials are bringing sweeping changes in the way humans interact with engineering devices. A myriad of state-of-the-art applications are based on novel ways to actuate on structures that respond under different types of stimulus such as light [81], temperature [33, 82], electricity [70, 21], changes in the pH [85] and magnetic fields [36, 24]. Among them, materials that respond to magnetic stimuli enable to remotely modify their mechanical characteristics and macroscopic shape. Such magneto-sensitive materials are usually composed of two phases: i) a continuous or carrier phase and ii) a discontinuous or dispersed phase embedded in the former. Regarding the carrier matrix, they are usually classified as magnetorheological fluids [3, 15, 69], ferrogels [23, 84] and magnetorheological elastomers [6, 5, 17, 28, 32, 49]. Magnetorheological elastomers (MREs) are composed of a vulcanized polymeric carrier matrix with magnetic particles embedded on fixed positions. The type of the magnetic particles plays an important role as it defines the reversibility or remanence of the magnetisation of the sample. In this way, MREs can contain two major sets of fillers, referred to as soft-magnetic magnetorheological elastomers (sMREs) and hard-magnetic magnetorheological elastomers (hMREs).

sMREs exhibit a change in their mechanical properties when an external magnetic field is applied [79]. However, when the field stops acting, such a change reverts to the original state, i.e., the magnetisation of the sample is lost. The emergence of hMREs changed the paradigm by allowing for sustained magnetic effects along time [65]. When magnetic particles with permanent magnetisation are used, the composite acquires novel magneto-mechanical properties with a wider array of degrees of freedom to design more complex responses [36, 46]. Contrary to sMREs, the magnetorheological (MR) effect of hMREs (i.e., structural stiffness resulting from magneto-mechanical couplings) depends on the relative orientation of the magnetic field with respect to the magnetisation of the particles. The stiffening is known to be larger when the field is applied in the same direction as the magnetisation of the particles (co-directional or direct stimulation) than when the field is applied in the opposite direction (anti-directional or reverse stimulation) [40]. In addition, stimulating with small anti-directional magnetic fields can even decrease the shear modulus of the hMRE. This leads to asymmetric hysteresis loops and large energy dissipation due to particles rotation. In general terms, the magneto-mechanical stiffening when using hard-magnetic fillers is less intense than with soft-magnetic ones (i.e., the magnetisation of hard-magnetic particles is usually smaller than that of soft-magnetic ones) [11]. The alignment of particles and formation of chain-like structures, as described in [78], is one of the underlying mechanisms that drive this phenomenon. hMREs, however, stand out not only

for their permanent magnetorheological stiffening, but also for major shape changes.

Unlike soft-magnetic structures, hard-magnetic ones have been proposed as ideal candidates when morphological changes, and not only changes in the magnetorheological properties, are desired [13]. Some authors have reported that the magneto-mechanical behaviour of the particles is the result of a competition between two phenomena [62, 66]. For small magnetic fields, the interphase behaviour is such that the magnetic fillers tend to rotate with the field. This leads to mechanical torques transmitted to the carrier matrix that, overall, result in macrostructural shape changes. However, when the particles are mechanically prevented to turn (e.g., when using harder matrices [66]) and the magnetic field intensity increases, the magnetic particles get re-magnetised. Such a consideration enables extremely soft MREs (i.e., matrix with low stiffness) as ideal candidates for novel applications, as the activation of the magneto-mechanical couplings occurs for low external magnetic fields [49, 34]. In the literature, end-of-pipe applications of hMREs are based on two major characteristics: i) the modification of their mechanical properties (i.e., MR Effect) and ii) macrostructural shape changes. Note that, contrary to sMREs that only express complex shape changes when there are gradients in the magnetic fields, hMREs can also express such complex changes in shape under uniform fields [7]. Smart actuators and sensors are based on the deformation that results from the internal torques [8, 38, 43, 41, 58, 80, 87, 83, 73]. Soft robotics, namely as bioengineering applications, are remotely actuated to perform complex and repeatable movements [19, 20, 22, 30, 35, 43, 45, 47, 55, 56, 77, 76, 86]. Also, hMREs have been used as multifunctional shape-changing structures, e.g., metamaterials and self-healing structures [29, 42, 48, 53, 68, 16] and for industrial applications such as damping systems and electrical machines [1, 52]. However, prior to the design of any functional application, an integrative magneto-mechanical characterization of the material is crucial.

Experimental and computational methods are used to gain knowledge about the macroscopic magneto-mechanical response of MREs. Typically, magneto-mechanical rheology is utilised to understand the viscoelastic behaviour of such structures. Modern magneto-mechanical rheometers allow for testing under different deformation modes such as shear [2, 18, 27, 71, 4], axial [12, 39, 54, 59] and free expansion modes [49]. In the case of hMREs, a setup that permits to magnetise the sample under a large enough external magnetic field is required. Frequently, electromagnets or impulse magnetisers are used to generate fields up to 5 T [38]. To help better understand all these deformation modes and magnetic phenomena, several theoretical approaches have been proposed. The Stoner-Wohlfarth model has been used to understand the magnetisation and magnetic hysteresis of single-domain small magnetic particles [72]. Microstructural-based models

have been reported to understand the underlying magneto-mechanical interactions, i.e., dipole-to-dipole and Zeeman interactions [25]. Also, energy-based phenomenological constitutive models can be found in [26], and full-field numerical homogenization modelling, in [51]. This latter approach provides understanding of microstructural mechanisms that govern the overall response from the consideration of the actual particle distribution and interactions with the matrix. In general terms, both experimental and computational regards are complementary to gain knowledge on the behaviour of hMREs [57]. However, experimental work is paramount to feed computational models.

Despite the existence of applications that, according to the function, require soft- or hard-magnetic powders [9, 10, 64], to the best of our knowledge there is still a lack of guidance for the selection of the magnetic fillers to be used for MREs and the final properties provided to the structure. To make such a decision, a good understanding of the multifunctional mechanisms of both soft- and hard-magnetic MREs is necessary. Contrary to sMREs, and as a unique feature of hMREs, it is of special interest the study of their behaviour during and after being permanently magnetised, not necessarily reaching magnetic saturation. Under such circumstances, it is essential not only the magnetorheological characterisation, but also the control of the shape of hMRE structures under magnetic fields and the influence of geometrical effects together with multifunctional mechanisms at the microscale. Although some relevant works on soft hMREs have been published [60, 67], to the best of the authors' knowledge there is still a gap of knowledge on extremely soft hMREs (stiffness lower than 10 kPa). Such a soft nature of the elastomeric matrix promotes large microstructural deformations within the MRE that can lead to remarkable macrostructural responses. Therefore, the need of deeper insights into the response of such structures and comprehensive comparison with the soft-magnetic counterparts is necessary to allow for the eventual design of novel applications.

The aim of this work is to provide guidance by an original comprehensive characterization of extremely soft hMREs tested under different deformation modes (shear, confined and free deformation) and to set a comparative framework with the soft-magnetic counterparts (tested under the same conditions) that were presented in [49]. To this end, section 2 describes the design conditions and manufacturing of the samples. In section 3, the results for shear rheology of the hMRE during the magnetisation process are first presented and compared with the soft-magnetic counterparts. Then, Section 4 presents the results from axially confined deformation experiments under magnetic field ramps, as well as free deformation tests. These last experiments are meant to explore microstructural mechanisms, their competition with macrostructural ones and their mechanical rate dependencies. Moreover, they provide insights into the control of the morphology of hMREs

by means of heterogeneous magnetic fields (i.e., not using the upper yoke of the magneto-rheological accessory) and geometrical effects. Finally, section 5 gathers a comprehensive discussion and conclusions. The outcome of this work suggests that each type of magnetic filler (soft-magnetic and hard-magnetic powder) endows MREs with different structural behaviours. The magnetorheological characterisation offers valuable information about rate and magnetic dependencies. Also, the results prove that the low stiffness of these MREs supports novel potential applications as magneto-mechanical interplays get activated from quite low magnetic thresholds, i.e., the transmission of the actions from the magnetic particles to the soft matrix is done with special "ease" with respect to stiffer MREs.

2. Materials and synthesis

The proposed hMRE is composed of an extremely soft elastomer for the continuous phase (carrier matrix) and hard-magnetic powder for the discontinuous phase (magnetic fillers). In the literature, extremely soft PDMS matrices have been scarcely used [24, 49, 44, 31]. In this work, the extremely soft elastomer Dowsil CY52-276 (DowSil, Midland, MI, USA) (PDMS) (stiffness below 10 kPa) was chosen to achieve magnetorheological stiffening and shape changes with small external magnetic fields. This PDMS is provided by the manufacturer in two phases (phase A and phase B), which get cross-linked in the curing process. To this end, and following the manufacturer recommendations, the phases were blended at the volume ratio 1:1. In what concerns the magnetic phase, this is made of NdFeB, with hard-magnetic properties, provided by Magnequench (MQP-S-11-9-grade powder, Neo Materials Technology Inc., Greenwood Village, Colorado, United States). The median diameter of the spherical-shaped particles conforming the powder is 35 - 55 μm, and full-permanent saturation magnetisation is achieved with fields above 1600 kA/m (see [72, 62] for a deeper characterisation of the magnetic powder). The magnetic powder was added to the matrix according to the volume fractions $\phi = \{0.1, 0.2, 0.3\}$. To prevent sedimentation of the fillers, the elastomeric phases and the mould were pre-heated at 80 ^{o}C for 2 min. Increasing the initial viscosity of the mixture during the addition of the magnetic powder guaranteed that its homogeneous distribution within the elastomeric matrix was preserved without deposition issues. Note that this is a main difference with the manufacturing methodology of sMREs, where the smaller size of the fillers (radius of $3.9 - 5$ μm) does not cause sedimentation phenomenon. The reader can find more detail on the methodology used for sMREs in a previous work by the authors [49]. Afterwards, the blend was cured in an oven at 80 ^{o}C for 2 h, the same as for sMREs. Then,

120 1 mm height and 20 mm diameter-wise cylindrical samples were cut with a die. As a final step, to produce pre-magnetised samples, virgin ones were exposed to an axial homogeneous magnetic field of 1000 mT. Fig. 1 summarises the procedure followed.

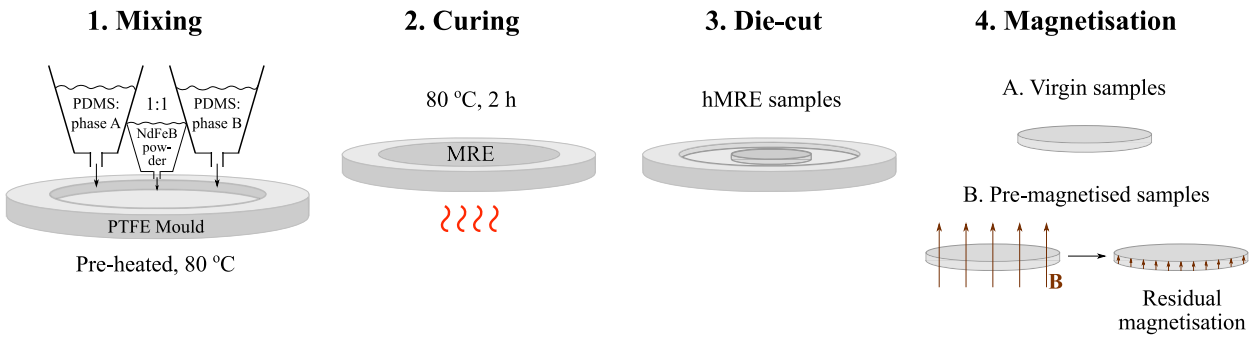

Figure 1. A scheme of the hMRE synthesis. The manufacturing methodology is composed of three steps: (1) blending of the components, i.e., the two phases of the pre-heated elastomeric matrix (phases A and B) and the hard-magnetic powder, previously poured into a pre-heated mould; (2) curing in an oven; (3) die-cutting of 1 mm height and 20 mm diameter samples; (4) the magnetisation of specimens with homogeneous magnetic fields.

The morphology of the matrix and distribution of the magnetic particles of both hard- and soft-magnetic MREs were assessed using field emission scanning electron microscopy (FESEM). To obtain cross-section
125 micrographs, virgin samples were frozen into liquid nitrogen prior to physical fracturing. The samples were coated with gold by using the Leica EM ACE600 (Leica, Wetzlar, Germany). Transversal micrographs were taken using a TENEO-LoVac (FEI, Hillsboro, Oregon) working at 5-10 kV. The results are presented in Fig. 2, where a homogeneous random distribution of the particles can be observed for both sMREs and hMREs.

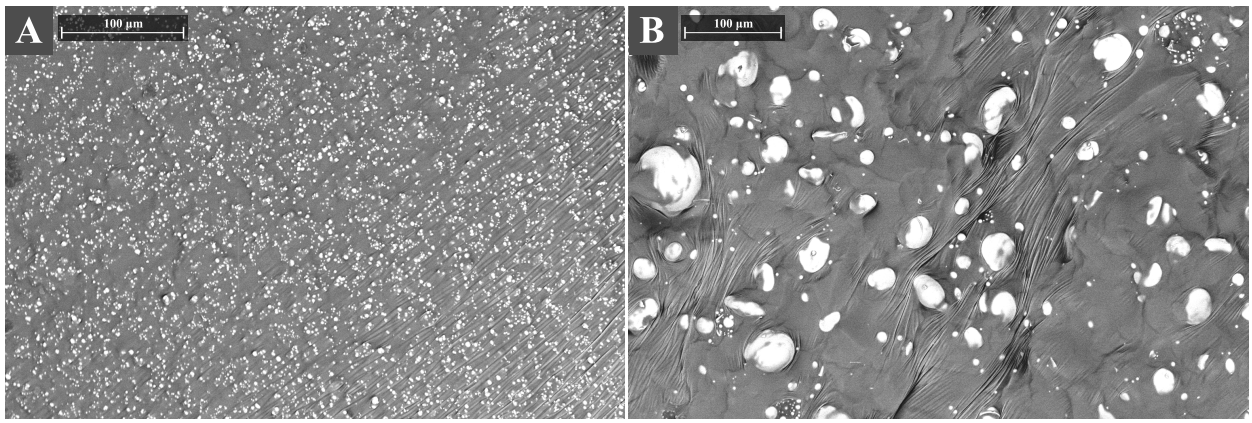

Figure 2. Field emission scanning electron microscopy (FESEM) images of the microstructural arrangement before magnetic actuation of: A) soft-magnetic MREs, and B) hard-magnetic MREs, both for a particles' content of 30 vol.%.

3. Magnetorheological characterisation under shear loading

Magneto-mechanical rheology was used to characterise the response of hMRE under coupled magneto-mechanical loading and shear deformation mode. To this end, a TA HR-20 rheometer with Magneto-Rheology Accessory from Waters TA Q600 (TA Instruments, New Castle, DE, USA) was utilised according to a previous work [49]. In the experiments conducted, magnetic actuation is such that the magnetic field is applied perpendicular to the sample, hence ensuring homogeneous fields in the testing region. After being exposed to large enough external magnetic fields, virgin hMRE samples acquire permanent magnetisation. Provided that the focus of the present study was to understand the response during the magnetisation process, and not only the behaviour after reaching full permanent magnetisation at saturation, partial remanent magnetisation rather than fully saturation magnetisation was intentionally pursued. This was done by the application of maximum fields under the value of 1600 kA/m (fully magnetising field given by the manufacturer). Note that if full saturation magnetisation is achieved, the remanent internal stresses become too large due to the extremely soft nature of the matrix. This would give raise to undesired extreme shape changes and magnetic interactions that could compromise the integrity of the composite. To observe the behaviour along the magnetisation process, different tests were performed under magnetic fields of 0 mT, 200 mT, 500 mT and 1000 mT on both virgin and pre-magnetised samples. This made possible to compare their structural response. As the amount of magnetic particles added to the MRE also plays an important role [24], the samples were manufactured and tested for magnetic particles' volume fractions of $\phi = \{0.1, 0.2, 0.3\}$. The results obtained for hMREs were compared with equivalent sMREs samples using soft-magnetic carbonyl-iron powder (CIP) (see [49] for more details).

3.1. Constant oscillatory shear

Hysteresis loops (also known as Lissajous figures) are representations meant to provide a straightforward measure of time-dependent phenomena (e.g., mechanical viscous dissipation), as well as the material behaviour under large deformation. A first array of experiments was designed for an angular amplitude of 0.05 rad. The angular velocity of the oscillations was chosen as 2 rad/s. In addition, the sticky nature of the sample prevents slippage at the sample-machine interfaces [74, 75, 72]. Shear hysteresis loops in Fig. 3 were obtained from constant angular oscillations plotting the azimuthal shear stress against shear strain at a radial coordinate $r = \frac{2}{3} r_{max}$, where $r_{max} = 20$ mm. Assuming a linear distribution of the torsion angle on

the rheometer axis (α) along the axial coordinate of the sample, and a linear distribution of the stress along the radial coordinate, the stress and strain for the representative coordinates are calculated, respectively, as:

$$\tau(M) = \frac{4M}{3\pi r_{max}^3}, \qquad \gamma(\alpha) = \frac{2}{3}\frac{\alpha r_{max}}{H}, \tag{1}$$

with H the height of the sample and M the torque on the rheometer's axis.

The results of the tests have lead to relevant findings. First, the MR effect (defined as $\frac{G'_{B=i}}{G'_{B=0}}$, with G' the shear storage modulus for a magnetic field B) is less pronounced when using hard-magnetic particles than soft-magnetic ones, with maximum values of approximately 4 times versus 30 times, respectively. hMREs, however, are able to keep this effect even in the absence of magnetic stimulation and, as it will be discussed in following sections, they are able to perform functional deformation modes. When actuating on virgin samples with external magnetic fields below 200 mT, hysteresis loops do not display any remarkable MR effect, even for the largest volume ratio of magnetic particles of 0.3. Fig. 4 clarifies the results from the loops in Fig. 3.a, by showing an initial range where the maximum shear stress does not depend on the magnetic field. From 500 mT on, however, the specimens reach larger maximum shear stresses (i.e., for 500 mT and 1000 mT fields). Such a threshold was not encountered when using soft-magnetic particles, i.e., the MR effect was noticeable for the smallest fields too, see Fig. 3.b. On the contrary, pre-magnetised hMRE samples display a different behaviour. In the absence of magnetic actuation, they reach larger stresses than virgin samples, and for fields below 200 mT, MR effect is also noticeable, see Fig. 4. As a final general remark, the more magnetic fillers added to the matrix, the stronger the magneto-mechanical effects are.

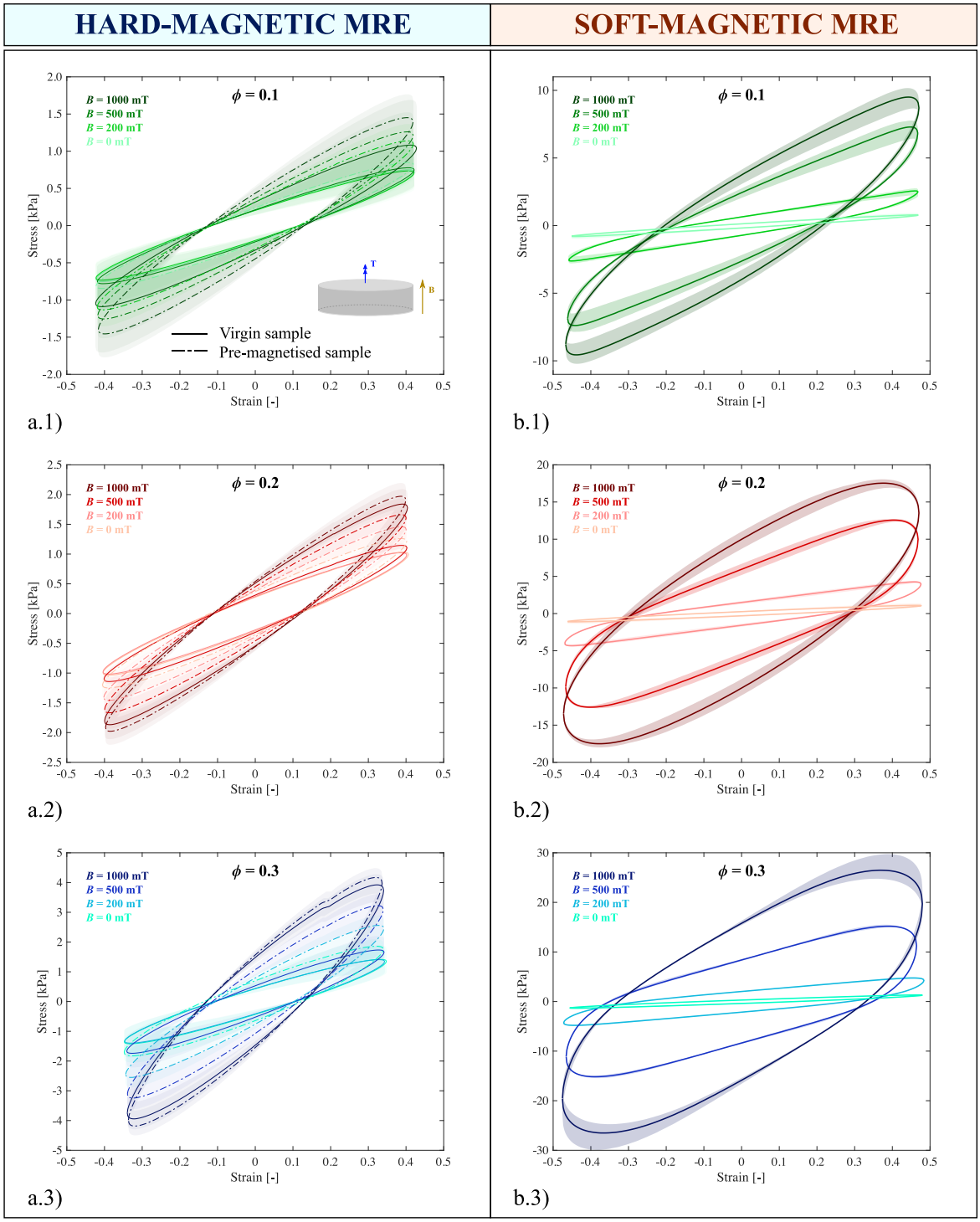

Figure 3. Comparison of the mechanical response of MREs under shear deformation with (a) hard-magnetic particles and (b) soft-magnetic particles (adapted from [49]). The experimental results from constant oscillatory shear tests are depicted for magnetic particles' volume fractions of $\phi = \{0.1, 0.2, 0.3\}$ and magnetic fields of $B = \{0, 200, 500, 1000\}$ mT. To account for the magnetic remanence, hard-magnetic MREs are tested twice: virgin samples and magnetised samples after a permanent magnetisation at 1000 mT (continuous and dashed line, respectively). Scatter areas are plotted around the mean curves computed from the three data sets obtained for the same testing conditions.

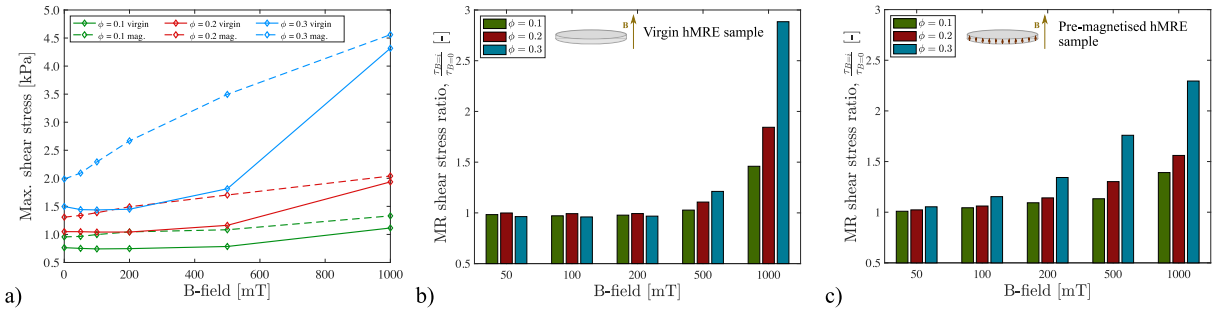

Figure 4. Effects of the permanent magnetisation of hMREs on the maximum shear stress of the hysteresis loops from the constant oscillatory shear experiments. (a) Curves for tests with magnetic particles' volume fractions of 0.1, 0.2 and 0.3 are plotted against the magnetic field intensity. Two curves for each volume fraction stand for the behaviour of virgin samples (continuous line) and pre-magnetised samples (abbreviated as mag.) after experiencing pre-magnetisation at 1000 mT (dashed line). (b-c) Magneto-rheological shear stress ratio, defined as the quotient between the maximum stress under magnetic actuation and the stress in the absence of external magnetic actuation, for (b) a virgin sample and for (c) a pre-magnetised sample.

3.2. Dynamic mechanical analysis (DMA) under shear deformation

To explore the relation between the viscoelastic response of hMREs and the mechanical excitation frequency, a second set of experiments was performed as frequency sweeps from 0.01 Hz to 10 Hz. Here, measures of the macrostructural stiffness were provided by means of the shear storage modulus (G'), shear loss modulus (G'') and loss factor $\tan\delta = \frac{G''}{G'}$, see Fig. 5.a, and Figs. A.1.a and A.2.a from the Appendix, for magnetic particles' volume fractions of 0.3, 0.1 and 0.2, respectively. Note that these moduli are determined by the linearisation of the material stiffness at small strain and within the linear viscoelastic region, i.e., tangent modulus. Moreover, magnetic fields of $B = \{0, 200, 500, 1000\}$ mT were applied on both virgin and pre-magnetised hMREs specimens. The effect of the non-zero magnetic coercivity of the hard-magnetic particles on the structural response of hMREs is shown by means of the curves for pre-magnetised samples (i.e., after previously magnetised at 1000 mT). The main findings are the following ones. First, the MR effect is stronger for increasing amounts of hard-magnetic particles. The MR effect for a magnetic actuation of 1000 mT, mechanical oscillation at 0.1 Hz, hMRE virgin samples, and particles contents of 10 vol.%, 20 vol.% and 30 vol.%, is 1.5, 2.1 and 3.0, respectively. For the pre-magnetised samples and for the different particles content, the MR effect is 1.5, 1.9 and 2.2, respectively. For a faster deformation, i.e., 10 Hz, the MR effect for the virgin samples is 1.5, 2.0 and 2.8, and for the pre-magnetised ones it is 1.4, 1.6 and 1.9, respectively for the particle contents considered. Second, for the intermediate fields of 200 mT and 500 mT, the MR effect for pre-magnetised samples significantly increases with respect to the MR effect of virgin samples. For 200 mT and quasi-static mechanical deformation, the MR effect of the virgin hMRE sample with 30 vol.% particles is 1.0, and 1.4 for the pre-magnetised sample. For 500 mT, the MR effect of the

virgin hMRE sample is 1.3, and 1.8 for the pre-magnetised sample. This tendency can be better visualised in Fig. 6, in which the shear storage modulus is plotted against magnetic field for a quasi-static (0.01 Hz) and a fast angular velocity (10 Hz). In this regard, the moduli of both virgin and pre-magnetised specimens merge to the same value when the field approaches 1000 mT.

When comparing the response of the hMREs with that of the sMREs, the MR effect is higher for the second ones. Overall, hMREs present a maximum MR effect of 3, whereas sMREs present a maximum of 12. Furthermore, for all the manufacturing and testing conditions of the hMRE, the loss factor monotonously increases with frequency, whereas for sMREs it is less dependent on the frequency. The response of hMRE is quite expectable, i.e., activation of viscoelastic mechanisms of the matrix at increasing deformation rates. For sMREs, however, the interactions between particles are much stronger (i.e., dipole-to-dipole interplays) due to their higher magnetisation and magnetic permeability. Such interactions lead to significant rearrangements in the particles' distribution and the generation of strong links between them, which eventually affect the viscoelastic response.

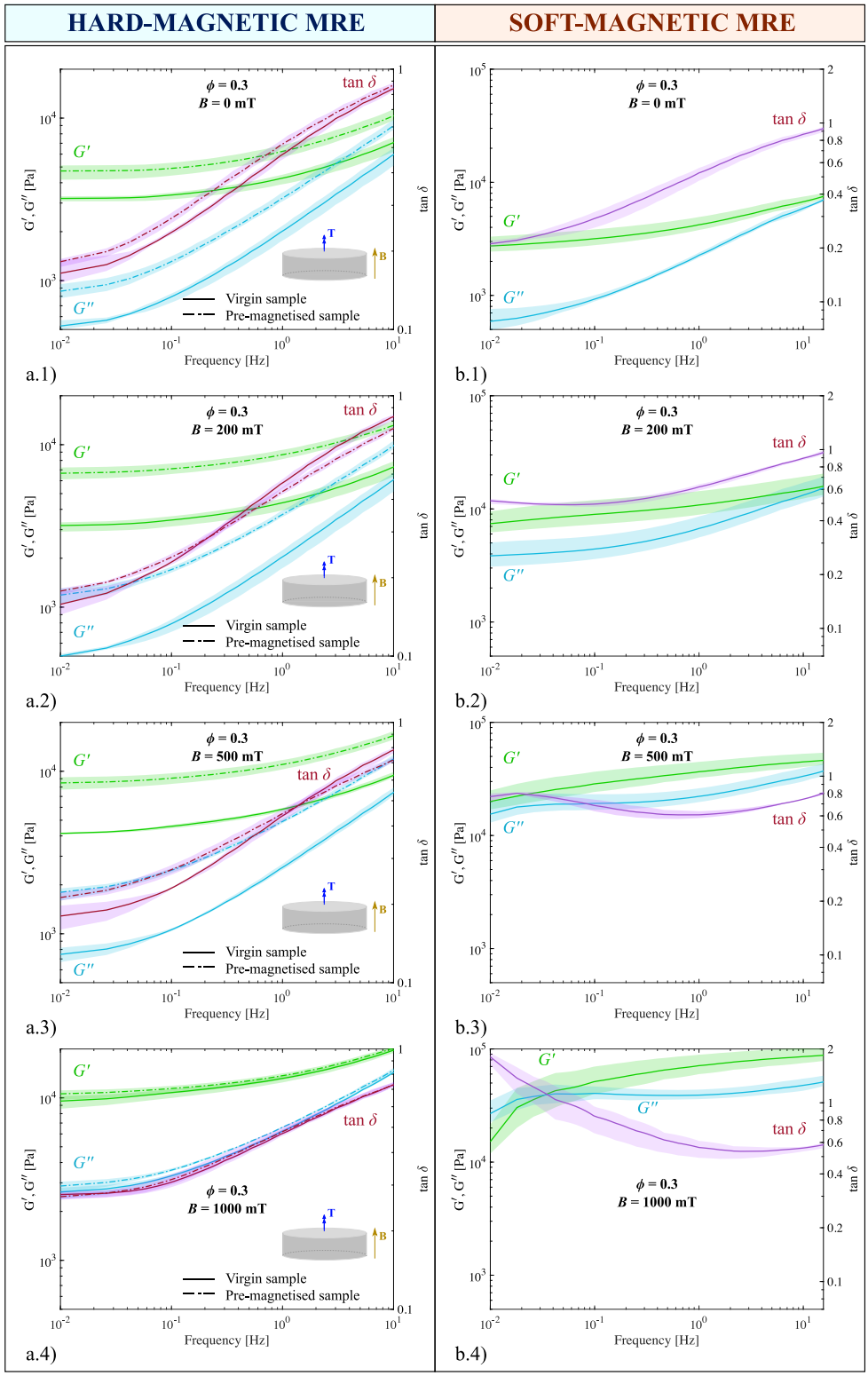

Figure 5. Dependence of the mechanical responses of MREs with the harmonic shear mechanical deformation for magnetic fields of $B = \{0, 200, 500, 1000\}$ mT and magnetic particles' volume fraction $\phi = 0.3$. Shear storage moduli (G'), loss moduli (G''), and loss factors ($\tan\delta$) obtained from frequency sweeps from 0.01 Hz to 10 Hz are compared for (a) hard-magnetic MREs and (b) soft-magnetic MREs (adapted from [49]). To account for the magnetic remanence, hard-magnetic MREs are tested twice: virgin samples and pre-magnetised samples after permanent magnetisation at 1000 mT (continuous and dashed lines, respectively). Scatter areas representing the variability of the experimental data sets are depicted around each mean curve.

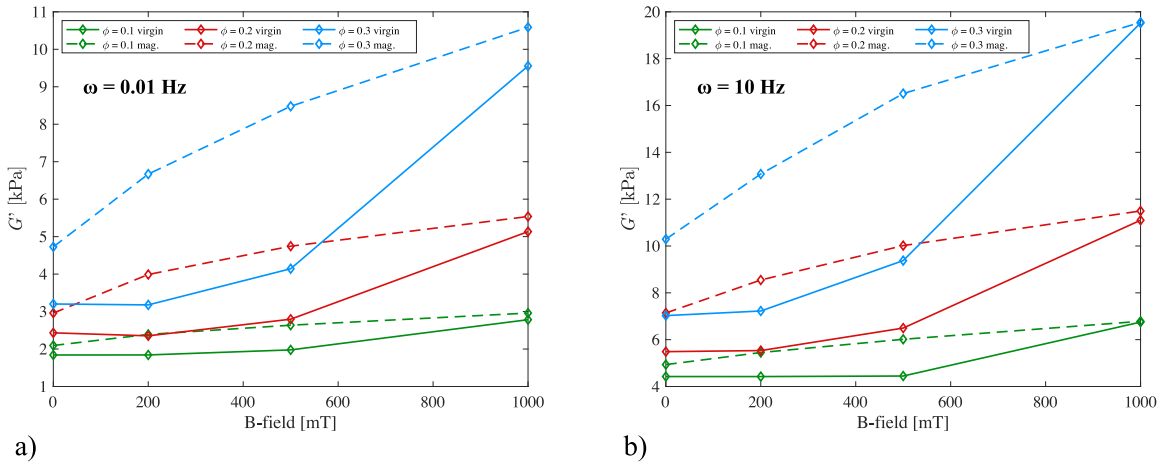

Figure 6. Effects of the permanent magnetisation of hMREs on the shear storage modulus for two extreme harmonic deformation velocities of (a) 0.01 Hz (quasi-static case) and (b) 10 Hz. Curves for tests with magnetic particles' volume fractions of 0.1, 0.2 and 0.3 are plotted against the magnetic field intensity. Two curves for each volume fraction stand for the behaviour of virgin samples (continuous line) and pre-magnetised samples (abbreviated as mag.) after experiencing re-magnetisation at 1000 mT (dashed line).

4. Magnetostriction dynamics of hMREs depending on residual magnetisation and geometrical effects

Even though the magnetorheological characterisation is vital to obtain valuable information about the modulation of the mechanical properties of MREs, the interest in extremely soft hMREs goes beyond the actuation on their mechanical properties [61]. The geometrical effects of these structures and their remarkable micromechanics (i.e., interplays between the magnetic particles and the matrix) enable them to perform complex deformations via magnetic actuation. To provide novel insights into the magnetostrictive behaviour of hMREs, this section presents: i) quantitative experiments measuring the magneto-mechanical response of hMREs subjected to fixed axial mechanical conditions and different external magnetic fields and ii) free deformation tests on samples with different geometries unveiling qualitative structural responses.

In what concerns the confined expansion experiments, magnetic field ramps were performed on virgin hMRE samples at the rate of 20 mT/s up to 1000 mT (direct magnetic actuation). Then, the field was kept constant for 75 s. Finally, the field was turned off for 50 s. In the meanwhile, the evolution of the axial force exerted on the upper plate of the rheometer was monitored. These experiments were done following the methodology reported in [49]. The pre-magnetised samples were tested following the same procedure but limiting the maximum magnetic field to 500 mT. The residual of the macroscopic samples after applying an external magnetic field of 1000 mT is 3 mT. Recalling the extremely soft nature of the matrix ($\sim$ 1 kPa),

a consequence is that such small magnetisation is enough to drive significant mechanical changes in the hMRE under external magnetic actuation. The use of the 500 mT is justified as it is sufficiently large to induce significant mechanical actuation, but small enough to not alter the residual magnetisation. Moreover, the magnetic actuation was performed in a reversed manner up to -500 mT (reverse magnetic actuation). To keep positive the axial force and prevent stretching the sample, an initial pre-compression of 0.5 N was imposed on all the tests. The results are grouped according to the magnetic profile applied and magnetisation state of the hMRE samples: magnetic field ramp up to 1000 mT on virgin specimens in Fig. 7.a and ramps up to +/-500 mT (direct and reverse fields) on pre-magnetised specimens in Fig. 7.b. Differences of the axial stress during the loading ramp can be found when comparing both the virgin and pre-magnetised samples. While for the virgin sample the curve is parabolic, for the magnetised specimen the load section is more linear. Another remark, when the magnetic actuation stops, is that the axial force decreases and becomes even smaller than the pre-compression at the beginning of the experiment. Then, it slightly increases. This is observed for the cases where the field is applied along the same direction as the magnetisation (i.e., "direct" fields). For the case of reverse magnetic actuation, almost no jump in the axial force occurs.

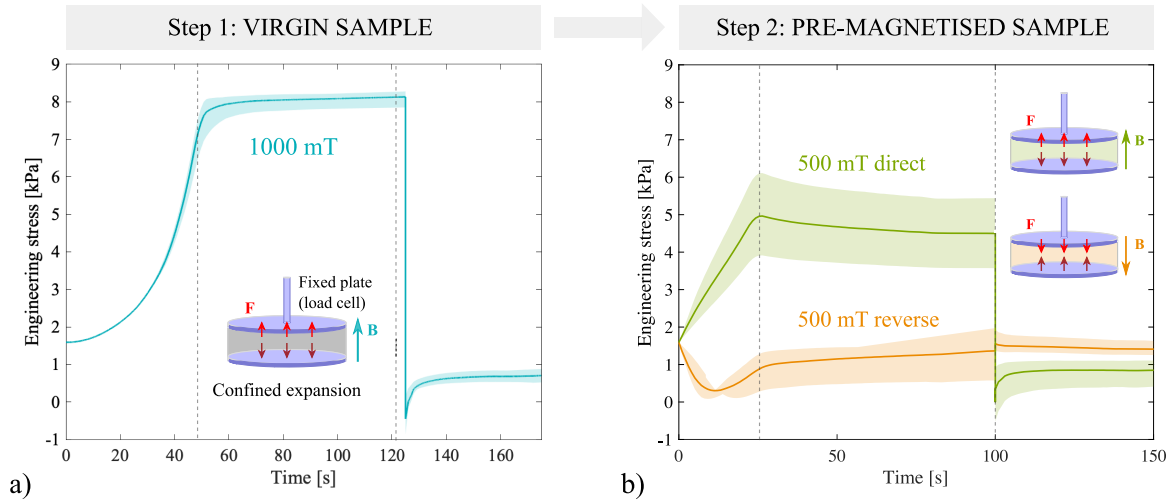

Figure 7. Time evolution of the axial stress of mechanically confined hMREs during magnetic ramps. In a), the magnetic actuation event of virgin specimens, which undergo a magnetic field ramp at a rate of 20 mT/s up to 1000 mT, that is then held until stabilisation and, finally, the magnetic actuation is turned off. In b), pre-magnetised samples were tested under the same procedure, but limiting the maximum magnetic field to 500 mT for both direct and reverse fields. Note that the same initial pre-compression of 0.5 N is applied for all the experiments to prevent that the axial force becomes negative, i.e., contraction of the sample.

Free deformation experiments were performed to analyse local-to-structural effects (i.e., geometrical effects) and the influence of rate dependences on them, see Fig. 8. Special attention has been paid along

the deformation processes to identify such local and structural mechanisms and to establish potential links with microstructural deformations (this will be further discussed in the following section). The tests were performed on different samples with bottom-up magnetisation (see the magnetisation procedure in Fig. 1). Fig. 8 presents the results according to the morphology of the hMRE specimens and the magnetic actuation conditions. These are shown as a collection of frames taken from the recorded videos. The time event was recorded using a CCD camera (Alvium, Allied Vision Technologies GmbH, Germany) with 25 mm focal length lens (Edmund Optics, Germany). Furthermore, to shed light on the shape-morphing capability of hMREs, the findings are additionally classified into microstructural and macrostructural-based mechanisms. First, small cylindrical samples of 4 mm diameter were prepared and tested under alternating magnetic fields (oscillatory fields with amplitude of 300 mT and null bias) at frequencies of 1 Hz and 10 Hz, see Fig. 8.a. The small dimension of the sample allowed the magnetic field to be homogeneous through all the specimen (the homogeneity of the field was checked by making use of a teslameter in vacuum conditions; thus, small heterogeneities are expected at the sample edges). When actuating on the hMRE specimens at 1 Hz, two effects are observed. On the one hand, when the field starts increasing in the reverse manner, the upper and lower edges of the specimen start twisting towards the middle plane of the sample. On the other hand, when the field becomes large enough, macrostructural effects become sufficiently strong to make the sample turn and align with the magnetic field. The process starts again as the field goes in the other direction. When increasing the oscillation frequency of the field to 10 Hz, however, weaker local deformations were observed. Afterwards, two larger structures were tested to study geometrical effects, i.e., a bending disk with 20 mm diameter and a rectangular cantilever-shaped torsion beam (20 mm length and 5 mm width), see Fig. 8.b. For the bending disk, the heterogeneous magnetic field reaches maximum values in the centre of the specimen and a macrostructural response governs the deformation of its peripheral regions, i.e., these outer domains tend to macroscopically align with the central axial magnetic lines. Note that we refer as heterogeneous fields to those generated by the coil system when its upper yoke is not used. On the contrary, homogeneous magnetic fields are those achieved with the use of the upper yoke, as done in the previous sections for the rheological characterisation. In what respect to the cantilever beam, it performs a structural rotation via torsion along its longitudinal axis and following the external field.

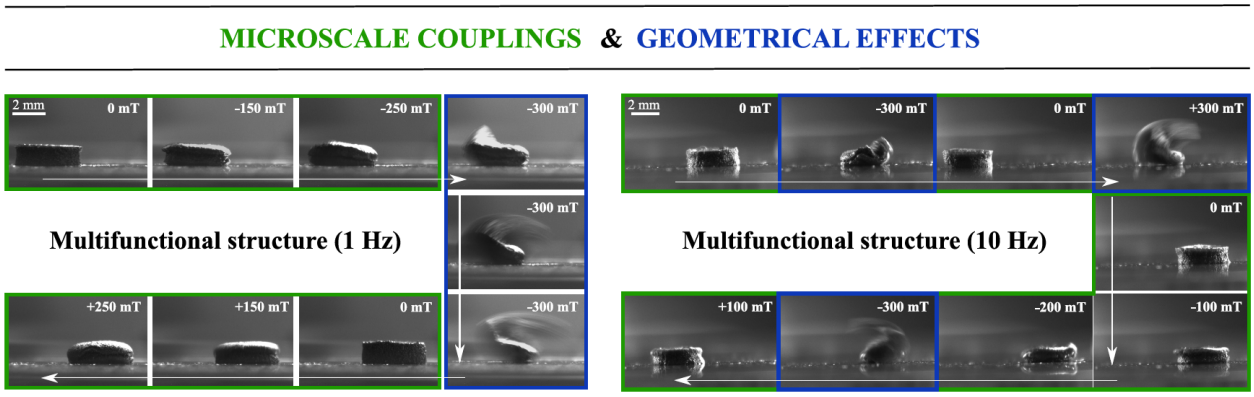

a. Influence of viscous effects. Competition between microscale-based mechanisms and structural interplays.

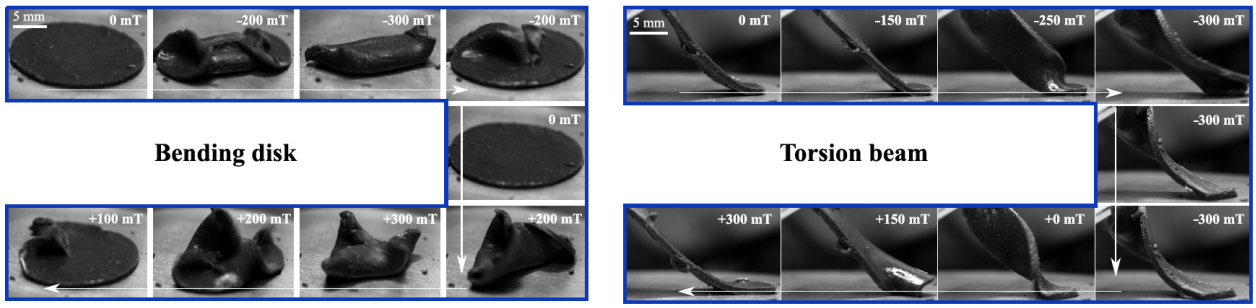

b. Influence of geometrical effects. Illustration of two functional applications of hMREs.

Figure 8. Tuning of the shape-changing behaviour of hMRE specimens by means of oscillatory magnetic stimulation and different initial geometries. The deformation modes that pre-magnetised hMRE samples undergo have been controlled by the application of harmonically-alternating magnetic fields. Low-diameter samples (i.e., 4 mm) were tested under field stimulation at (a.1) 1 Hz and (a.2) 10 Hz. Nine frames from recorded videos are shown for each case. In (b.1), the deformation scene of a larger (i.e., diameter of 20 mm) unveils macrostructural deformation modes. Finally, in (b.2), an alternative beam-shaped specimen undergoes torsion deformation.

The macrostructural response of hMREs is determined by the nature of the mechanisms that develop at the microscale, namely the magnetic interactions between the magnetic particles and the mechanical interactions between these and the carrier matrix. In this regard, Fig. 9 illustrates the connection between the macrostructural functional deformation mode and the underlying microstructural mechanisms for a pre-magnetised hMRE. Three cases are described. First, when the structure is magnetically actuated in the same direction that it is pre-magnetised, the particles tend to align forming chain-like structures. This mechanism produces the macrostructural expansion of the hMRE, and it relates to the results in Fig. 7 for the confined expansion experiments under direct magnetic actuation. Second, a perpendicular magnetic actuation with respect to the pre-magnetisation leads to macrostructural bending. At the microscale, the particles try to

rotate and align its magnetisation with the external field. The results for the bending disk and torsion beam under free deformation in Fig. 8.b relate to this mechanism. Finally, co-linear but reverse magnetic actuation produces symmetric twisting of the structure. Due to the extremely soft nature of the matrix, the particles
285 tend to rotate and align with the external field, introducing microstructural torques in the hMRE. Such a mechanism is observed on the multifunctional structure in Fig. 8.a.

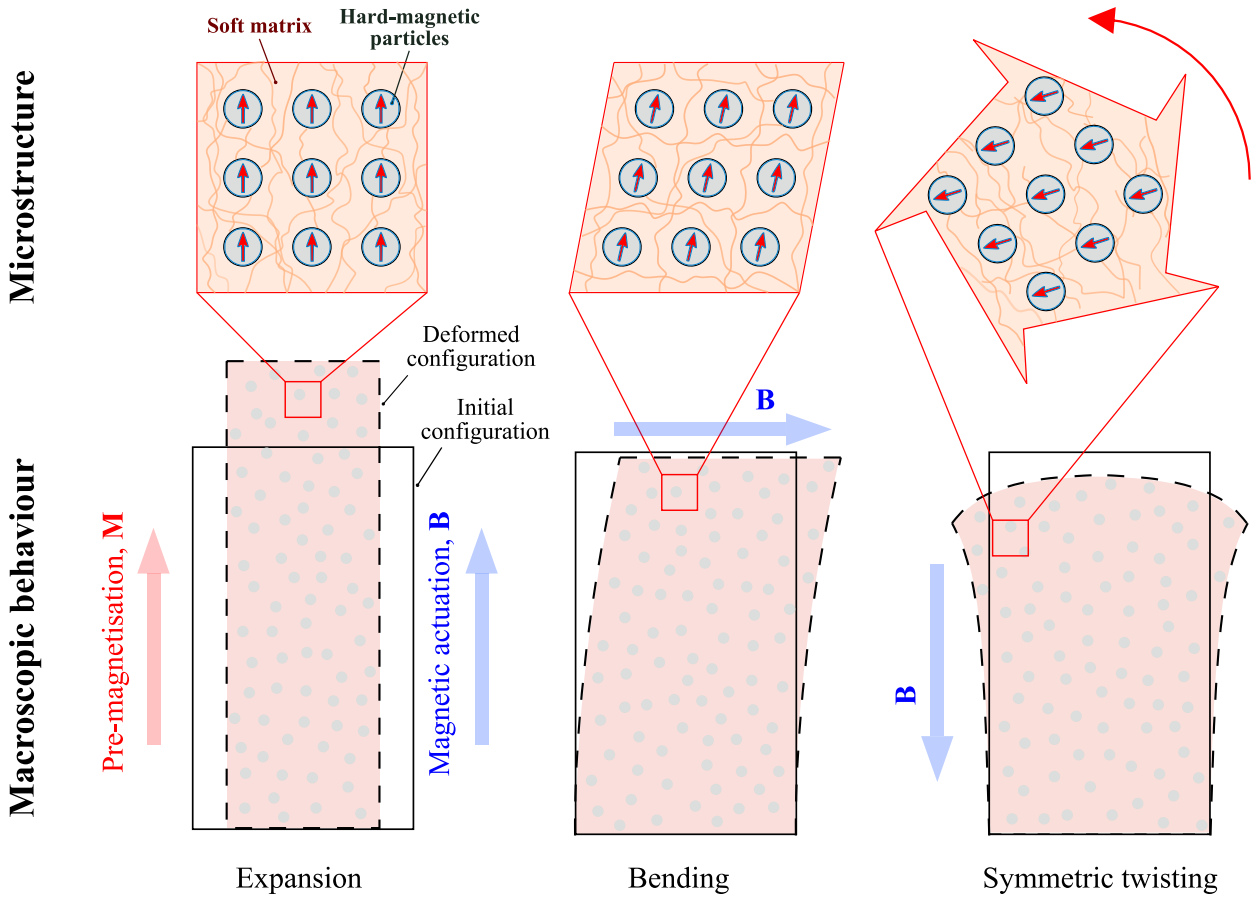

Figure 9. Schematic representation of the microscopic and macroscopic magneto-mechanical deformation mechanisms in hMREs under different magnetic actuation scenarios. (Left) Structural response under magnetic actuation parallel to the remanent magnetisation and with the same orientation (direct actuation). Under this condition, the particles tend to align forming chain-like structures, leading to an overall expansion. (Centre) Structural response under magnetic actuation perpendicular to the remanent magnetisation. Under this condition the particles try to rotate and align its magnetisation with the external field. This leads to overall bending. (Right) Structural response under magnetic actuation parallel to the remanent magnetisation and opposite orientation. Under this condition, and due to the extremely soft nature of the matrix, the particles try to rotate and align with the external field introducing microstructural torque in the hMRE.

5. Discussion

The experimental campaign presented in this work promotes a comprehensive discussion based on three major pillars: the magneto-mechanical rheological characterisation of extremely soft hMREs at different magnetisation conditions, the actuation to perform complex (local and structural) deformation modes and the comparison with their soft-magnetics counterparts. Special attention has been put on the study of the effects of residual magnetisation below saturation of such structures, i.e., not reaching full saturation magnetisation. To this end, the mechanical response of the samples under shear loading is discussed from the results in Sections 3.1 and 3.2. Afterwards, the behaviour of internal magneto-mechanical couplings of hMREs is understood from the evolution of the axial force from confined deformation tests in Sec. 4. Finally, free deformation experiments are taken to provide a better understanding on how the magnetic inclusions transmit magnetic torques to the elastomeric matrix, together with chain formation mechanisms, leading to macrostructural shape changes of the hMRE.

Regarding the rheological behaviour of extremely soft hMREs, permanent magnetisation leads to increased stiffness in the absence of external magnetic stimulation. To clearly understand the effects of the permanent magnetisation, Figs. 4 and 6 show, respectively, curves with the evolution of the maximum shear stresses of the hysteresis loops and the quasi-static storage modulus for different magnetic particles' volume fractions and magnetic fields, for both virgin and pre-magnetised hMRE samples. When the external magnetic field is turned off, internal magnetic interactions between the magnetic particles and the elastomeric matrix still remain. Also, the more magnetic particles, the larger the apparent (homogenised) permanent magnetisation. This fact explains the relative stiffness increase between virgin and pre-magnetised samples with increasing particles volume fraction, both under the action of external magnetic fields or in the absence of them. In addition, the relative stiffness increase reduces to zero at 1000 mT, expectable as the MRE got magnetised at 1000 mT. When comparing the results between hMREs and sMREs, see Fig. 3, it is clear that the MR effect is larger for the soft-magnetic version (around 7 times larger). This is so because the saturation magnetisation and magnetic susceptibility of hard-magnetic MQP-S-11-9-grade powder are smaller than those of CIPs, see magnetisation curves in the Appendix, Fig. A.3, adapted from [11]. Overall, hMREs lose the intense MR stiffening of sMREs but gain the capability to achieve it in the absence of magnetic fields.

Non-symmetric macrostructural responses are observed for direct (along magnetisation direction) and reverse (contrary to magnetisation direction) magnetic fields on pre-magnetised hMRE samples tested in confined deformation experiments. Following the evolution of the axial force exerted by the sample on the fixed

plates, see Fig. 7, valuable information about the magnetisation process is harvested. The initial magnetic actuation up to 1000 mT yields an initial parabolic increase in the stress. This can be explained by the quadratic dependence of internal magnetic stress on the externally applied magnetic field [14, 25, 49]. The abrupt decrease in the stress when stopping the magnetic actuation and the subsequent relaxation unveils internal viscous mechanisms. As these stresses go below the initial axial force, we believe that the specimen internal deformation mechanisms are not reversible. In other words, the microscopic configuration of virgin and pre-magnetised hMREs would be different. When observing the results for the second stimulation step (i.e., direct and reverse fields up to 500 mT) the same finding can be reported. Hence, this behaviour is not due to the permanent magnetisation of the magnetic powder but due to varying microstructural arrangements also under weaker magnetic actuation. Finally, regarding the effect of the magnetisation direction, the non-symmetrical curves for the direct and reverse fields suggest that reversing the magnetic field produces a decrease of the axial force (i.e., confined compression) rather than an increase. In addition, such a decrease is smaller in magnitude than the increase for the direct field. A further finding related to such a reverse stimulation is that the evolution of the axial force during the application of the magnetic field ramp is not monotonous. Such findings under reverse magnetic actuation can be understood as the result of local rearrangements of the particles that were aligned with the magnetisation field (direct magnetic actuation). When the sense of the field changes, we believe that local rearrangements of the particles occur until they align with the new field. This transient mechanism would end in a microstructural stabilization where interactions between different domains of the hMRE structure govern the structural response.

Related to the latter discussion, another important observation from Fig. 7 relates to the transient stress evolution that occurs once the maximum magnetic field is reached. On virgin samples, the steady state is quickly reached, suggesting negligible relaxation effects. However, the tests conducted on pre-magnetised samples present a transient stress response indicating significant relaxation within the MRE. To explain these results, we suggest the existence of two main microstructural deformation mechanisms. First, the application of an external magnetic field on virgin samples results in dipole-to-dipole interactions leading to the formation of chain-like microstructures and the subsequent expansion of the MRE (i.e., increase in confined stress). Fig. 9 illustrates the expansion deformation mode. Then, when switching off the external magnetic field, the dipole-to-dipole interactions are relaxed leading to a re-accommodation of the particles within the MRE, which present a given residual magnetisation. Second, when applying a magnetic field on pre-magnetised samples, the previously mentioned dipole-to-dipole interactions are combined with micro-torques due to

Zeeman effect [25]. These torques induce high local deformations around the particles resulting in a stronger relaxation response. In addition, the orientation of the particles' residual magnetisation follows the rotation of the particles during such micro-relaxations, introducing time-varying microstructural equilibrium states. To elaborate on this behaviour, deformation tests under free boundary conditions are discussed hereafter.

Free deformations of hMRE specimens unveil the underlying mechanisms that govern the interaction between the elastomeric and magnetic particles phases. In Fig. 8.a, it can be seen that, when the reverse magnetic field is applied, the upper edges get twisted in a symmetric fashion. This suggests that the structural response is initiated at the microstructural level by translating microscopic deformation mechanisms into synergistic effect at the macroscale. We believe that such a complex morphological change unveils microscale transmission mechanisms of the magnetic torques on the particles to the matrix (this latter balances such mechanical actions). From a microstructural point of view, the magnetic particles are embedded in the carrier matrix. Under the application of a magnetic field, they can respond alternatively by: i) rotating and orientating along the direction of the field or ii) re-magnetising by reversion of the orientation of the magnetisation. Which phenomenon occurs is determined by the stiffness of the matrix. For soft matrices and small magnetic fields, the particles turn after the field, and for larger fields and stiffer matrices, they get re-magnetised [62, 66]. Fig. 9 provides an illustration of the twisting deformation mechanism governed by the transmission of torques form the particles to the matrix. Moreover, the deformation rate determines the response of the specimen. When the oscillation of the magnetic field is increased, local deformation of the sample (i.e., twist of the edges) plays a minor role. This is so because the faster the actuation, the stiffer the sample becomes and, therefore, the more difficult for the particles to turn and orient. Such an effect could lead to an eventual microstructural collapse, as reported in [49].

When the geometry of the specimens is larger, see the bending disk and torsion beam in Fig. 8.b, instead being local deformation the governing mechanisms, macrostructural changes in the shape appear as major effect on the material. Depending on the geometry of the specimen, the interaction between local domains of the hMRE can be tuned to achieve different complex deformation modes. Note that this type of deformation for homogeneously pre-magnetised specimens is only achievable by means of heterogeneous magnetic fields. For the case of the disk, bending of the outer regions occurs, and for the case of the torsion beam, the entire structure tends to turn 180 degrees to align with the imposed external field. Fig. 9 provides an illustration of the bending deformation mode. These non-trivial deformation modes can relate to classifications reported in the literature, according to the movements, as deflections, elongations, contractions, coiling,

crawling and jumping [7]. As a general concern, note that full saturation magnetisation of the hMRE instead of partial magnetisation (i.e., according to the manufacturer, fully magnetisation is reached for a field of intensity 1600 kA/m) would yield permanent deformations larger than the ones obtained in Fig. 8. For such a soft matrix, this would hinder the control and functional response of such hMREs. Therefore, we accept the maximum field of 1000 mT to be large enough for the activation of magneto-mechanical couplings and the functional application of the hMRE.

In addition to the previous considerations, some additional points should be taken into account to close the entire image provided in this work. First, particle size is a major factor determining the magneto-mechanical response of hMREs. Some authors reported that larger magnetic particles have a greater capability to overcome the elastic forces of the matrix when trying to align with the external magnetic field [63]. Therefore, the smaller the hard-magnetic particles, the closer to soft MREs behaviour; and the bigger the particles, the larger the tendency to rotate. When the matrix is soft enough, the micro-rotations of the particles are stronger than their transmission to the entire structure. For this reason, using smaller particles in extremely soft matrices could increase the effectiveness of torque transmission. In our work, the hard-magnetic particles used are one order magnitude bigger than the soft ones. Stepanov et al. [66] reported that stiffer matrices have a better capability to confine the fillers, i.e., prevent their turning; and softer matrices allow for the particles to turn. In this last case, which is the one of our extremely soft hMREs, the hysteresis phenomenon on the magnetisation loops with the imposed magnetic field has been reported to be less accused. As the particles turn, no re-magnetisation is reached. Note that this was verified measuring the same residual magnetisation of the pre-magnetised samples before and after the experiments. Therefore, the larger the storage modulus of the hMRE, the larger the coercive force. As future work, the results obtained herein could be contrasted with stiffer hMREs (i.e., stiffer carrier matrices) and under magnetisation beyond 1000 mT until saturation. Moreover, a further interesting point to explore would be the magnetisation of hMREs in a heterogeneous manner. In this way, it would be possible to address shape changes with homogeneous external magnetic fields, as recently done for stiffer hMREs by Zhao and co-authors [88].

6. Conclusions

The extremely soft nature of the matrix of the soft hMREs conceptualised in this work and their capability to acquire permanent magnetisation endow them with remarkable features. The magnetorheological charac-

terisation performed in this work allows the quantitative discussion and comparison with sMREs. It is found that the MR effect is weaker in hMREs than in sMREs (approximately, 7 times smaller) but, instead, they have the capability to retain the magnetorheological stiffening in the absence of an external magnetic stimulation. Provided the extremely soft nature of these structures, a significant magneto-mechanical coupling occurs at low external magnetic fields (below 1000 mT). Furthermore, soft hMREs have been shown to be suitable for tuning complex morphological changes by two ways: acting on local deformation mechanisms (i.e., microscale interplays between the matrix and magnetic particles) and tuning macroscopic geometrical interplays. The former concerns the transmission of torques from the particles to the matrix, as they tend to align with the external magnetic field. The latter, however, is based on the interaction between different domains of the hMRE structure and is actuated via heterogeneous external magnetic fields.

Overall, we facilitate links between the microstructure and the macrostructure through specific experiments that are reported herein for the first time on hMREs. We highlight the "confined tests" presented in Fig. 7, where the samples are mechanically constrained at the macroscale. The quasi-incompressible nature of the material and the axisymmetric conditions during the tests imply that the material does not deform macroscopically. However, our experimental system provides a macroscopic measurement by means of axial stress when we applied an external magnetic field. This is a clear demonstration of how microstructural mechanisms lead to a macroscopic response. Then, the experiments under free mechanical boundary conditions and the application of external magnetic fields present a macrostructural deformation as a result of the microstructural mechanisms (particle interactions due to dipole-to-dipole interactions, Zeeman effect, re-arrangement of particle distribution, etc.).

The insights presented in this work are of high interest for understanding the role of magneto-mechanical coupling in hMREs and motivate future computational approaches. In addition, the better comprehension of the hMRE characteristics opens new potential applications. In the bioengineering field, a recent paper by Moreno-Mateos et al. [50] shows the potential of sMREs as biological substrates to influence cellular processes. The incorporation of hard-magnetic particles to these substrates would enable transitions in their mechanical performance that can be kept without the need of sustaining external magnetic fields. Another interesting application would consist in mixing hard- and soft-magnetic particles within the same MRE to provide smart structures whose magneto-mechanical coupling can exhibit the benefits of each particle type and even potential synergistic effects.

Acknowledgement

The authors acknowledge support from the European Research Council (ERC) under the European Union's Horizon 2020 research and innovation programme (grant agreement No. 947723, project: 4D-BIOMAP). The authors acknowledge support from MCIN/ AEI /10.13039/501100011033 under Grant number PID2020-117894GA-I00. MAMM acknowledges support from the Ministerio de Ciencia, Innovacion y Universidades, Spain (FPU19/03874) and DGG acknowledges support from the Talent Attraction grant (CM 2018 - 2018-T2/IND-9992) from the Comunidad de Madrid. MH acknowledges the funding through an EPSRC Impact Acceleration Award (EP/R511614/1).

Appendix A. Supplemental Results

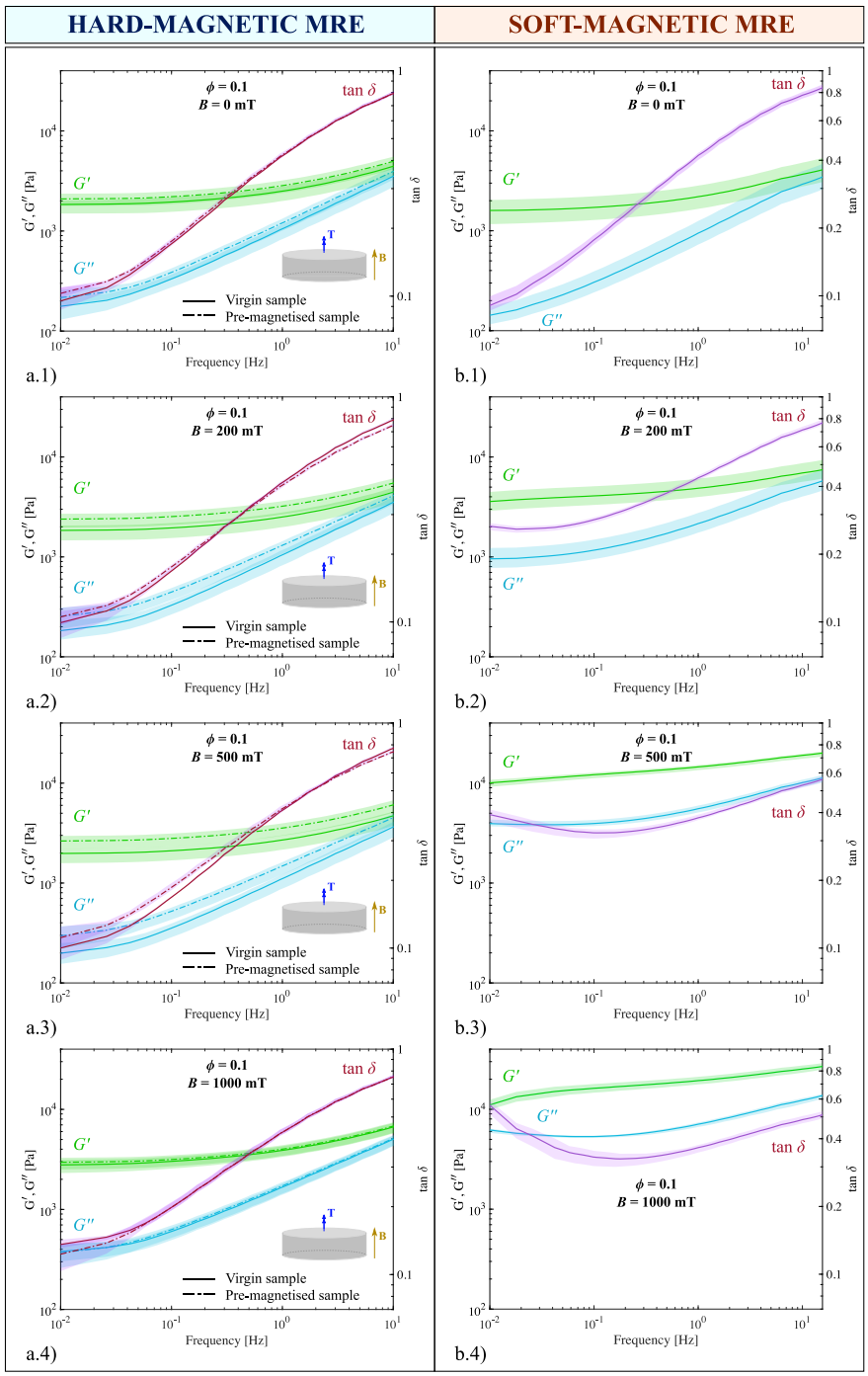

Figure A.1. Dependence of the mechanical response of MREs with the harmonic shear mechanical deformation for magnetic fields of $B = \{0, 200, 500, 1000\}$ mT and magnetic particles' volume fraction $\phi = 0.1$. Shear storage moduli (G'), loss moduli (G''), and loss factors ($\tan\delta$) obtained from frequency sweeps from 0.01 Hz to 10 Hz are compared for (a) hard- and (b) soft-magnetic MREs. To account for the magnetic remanence, hard-magnetic MREs are tested twice: virgin samples before permanent magnetisation at 1000 mT and pre-magnetised samples after permanent magnetisation (continuous and dashed line, respectively). Scatter areas representing the variability of the experimental data sets are depicted around each mean curve.

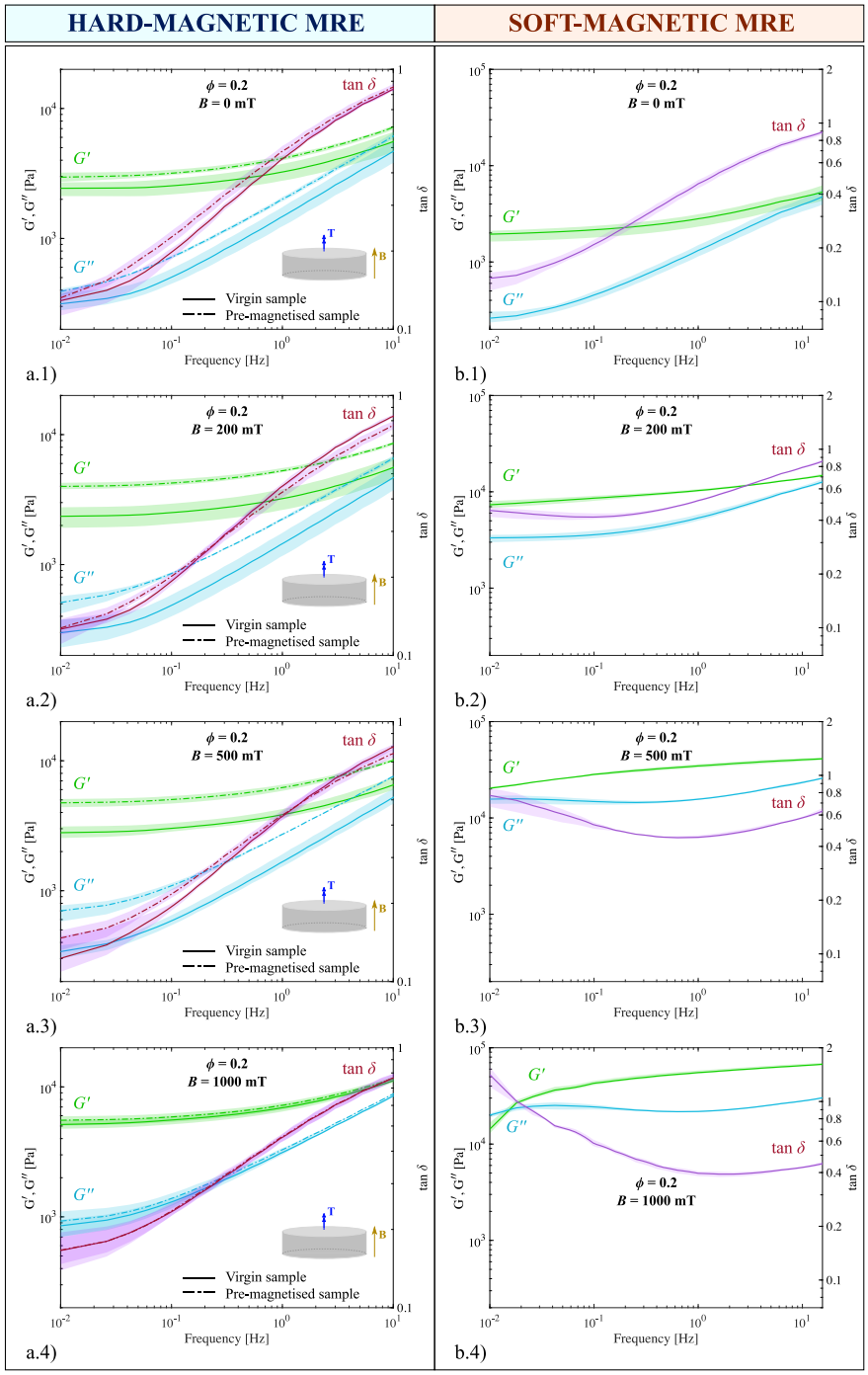

Figure A.2. Dependence of the mechanical response of MREs with the harmonic shear mechanical deformation for magnetic fields of $B = \{0, 200, 500, 1000\}$ mT and magnetic particles' volume fraction $\phi = 0.2$. Shear storage moduli (G'), loss moduli (G''), and loss factors ($\tan\delta$) obtained from frequency sweeps from 0.01 Hz to 10 Hz are compared for (a) hard- and (b) soft-magnetic MREs. To account for the magnetic remanence, hard-magnetic MREs are tested twice: virgin samples before permanent magnetisation at 1000 mT and pre-magnetised samples after permanent magnetisation (continuous and dashed line, respectively). Scatter areas representing the variability of the experimental data sets are depicted around each mean curve.

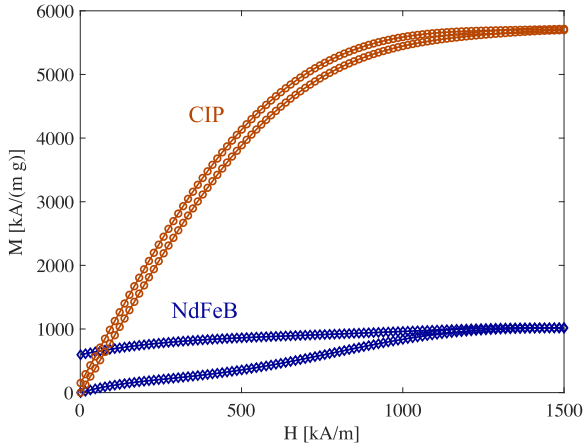

Figure A.3. Magnetisation curves for BASF carbonyl iron powder (CIP) and Magnequench NdFeB MQP-S-11-9 (adapted from [11]).

References

[1] Abramchuk S, Kramarenko E, Grishin D, Stepanov G, Nikitin LV, Filipcsei G, et al. Novel highly elastic magnetic materials for dampers and seals: Part II. Material behavior in a magnetic field. Polym Adv Technol 2007;18:513–8.

[2] Agirre-Olabide I, Berasategui J, Elejabarrieta MJ, Bou-Ali MM. Characterization of the Linear Viscoelastic Region of Magnetorheological Elastomers. Journal of Intelligent Material Systems and Structures 25, no. 16 2014: 2074â€“81. https://doi.org/10.1177/1045389X13517310.

[3] Asiaban R, Khajehsaeid H, Ghobadi E, Jabbari M. New magneto-rheological fluids with high stability: Experimental study and constitutive modelling. Polymer Testing 2020.106512. ISSN 0142-9418. https://doi.org/10.1016/j.polymertesting.2020.106512.

[4] Atul Narayan SP, Palade, L.I. Modeling Payne effect with a framework of multiple natural configurations. International Journal of Engineering Science. Volume 157 2020. 103396. ISSN 0020-7225. https://doi.org/10.1016/j.ijengsci.2020.103396.

[5] Bastola AK, Mokarram H. A Review on Magneto-Mechanical Characterizations of Magnetorheological Elastomers. Composites Part B: Engineering 2020: 108348. https://doi.org/10.1016/j.compositesb.(2020).108348.

[6] Bastola AK, Hossain M., Enhanced performance of core-shell hybrid magnetorheological elastomer with nanofillers. Materials Letters, Volume 297, 2021, 129944.

[7] Bastola, A. K., Hossain, M. (2021). The shape – morphing performance of magnetoactive soft materials. Materials & Design, 211, 110172. https://doi.org/10.1016/J.MATDES.2021.110172

[8] Becker TI, Zimmermann K, Borin DY, Stepanov GV, Storozhenko PA. Dynamic response of a sensor element made of magnetic hybrid elastomer with controllable properties. J Magn Magn Mater 2018;449:77–82.

[9] Borin, D., Stepanov, G., Dohmen, E. Hybrid magnetoactive elastomer with a soft matrix and mixed powder. Arch Appl Mech 89, 105â€“117 (2019). https://doi.org/10.1007/s00419-018-1456-9.

[10] Borin D, Stepanov G. Magneto-mechanical properties of elastic hybrid composites. 2019.

[11] Borin DY, Odenbach S, Stepanov GV. Stress induced by the striction of hybrid magnetoactive elastic composites. Journal of Magnetism and Magnetic Materials, Volume 470, 2019, Pages 85-88, ISSN 0304-8853, https://doi.org/10.1016/j.jmmm.2017.12.072.

[12] Borin DY, Stepanov GV, Odenbach S. Tuning the tensile modulus of magnetorheological elastomers with magnetically hard powder. 2013. Journal of Physics: Conference Series.

[13] Böse H, Hesler A, Monkman G. Magnetorheologische Kompositmaterialien mit hartmagnetischen Partikeln, Verfahren zu deren Herstellung sowie deren Verwendung. - Deutsche Patent DE 10 2007 028 663 A1. Priority: 21.06.2007. European Patent EP 2 160 741 B1 Granted: 17.08.2011.

[14] Bustamante R, Shariff MHBM, Hossain M. Mathematical formulations for elastic magneto-electrically coupled soft materials at finite strains: Time-independent processes, International Journal of Engineering Science, 2021 159:103429.

[15] Mahesh Chand, Ajay Shankar, Avinash Pratap Singh, Mohan Chandra Mathpal, Rajendra Prasad Pant, Jerome Deperyot. Mechanism of chain formation under shearing forces in magneto-rheological fluids, Materials Today: Proceedings, Volume 47, Part 8, 2021, Pages 1575-1579, ISSN 2214-7853, https://doi.org/10.1016/j.matpr.2021.03.675.

[16] Charles ADM, Rider AN, Brown SA, Wang CH. Multifunctional magneto-polymer matrix composites for electromagnetic interference suppression, sensors and actuators. Progress in Materials Science. Volume 115, 2021. 100705. ISSN 0079-6425. https://doi.org/10.1016/j.pmatsci.2020.100705.

[17] Chavez J, Ziolkowski M, Schorr P, Spieß L, Böhm V, Klaus Zimmermann, A method to approach constant isotropic permeabilities and demagnetization factors of magneto-rheological elastomers, Journal of Magnetism and Magnetic Materials, Volume 527, 2021, 167742, ISSN 0304-8853, https://doi.org/10.1016/j.jmmm.2021.167742.

[18] Dargahi A, Sedaghati R, Rakheja S. On the properties of magnetorheological elastomers in shear mode: Design, fabrication and characterization. Composites Part B: Engineering. Volume 159, 2019. Pages 269-283. ISSN 1359-8368. https://doi.org/10.1016/j.compositesb.2018.09.080.

[19] Dong X, Lum GZ, Hu W, Zhang R, Ren Z, Onck PR, et al. Bioinspired cilia arrays with programmable nonreciprocal motion and metachronal coordination. Sci Adv 2020;6(45):eabc9323.

[20] Son D, Ugurlu MC, Sitti M. Permanent magnet array–driven navigation of wireless millirobots inside soft tissues. Science Advances 2021. https://doi.org/10.1126/sciadv.abi8932

[21] dos Santos CR, Pacheco DRQ, Taha HE, Zakaria MY. Nonlinear modeling of electro-aeroelastic dynamics of composite beams with piezoelectric coupling. Compos Struct 2021;255:112968.

[22] Eshaghi M, Ghasemi M, Khorshidi K. Design, manufacturing and applications of small-scale magnetic soft robots. Extreme Mech Lett 2021;44:101268.

[23] Ganguly S, Margel S. Remotely controlled magneto-regulation of therapeutics from magnetoelastic gel matrices, Biotechnology Advances, Volume 44, 2020, 107611, ISSN 0734-9750, https://doi.org/10.1016/j.biotechadv.2020.107611.

[24] Garcia-Gonzalez, D., Moreno MA, Valencia L, Arias A, Velasco D. Influence of Elastomeric Matrix and Particle Volume Fraction on the Mechanical Response of Magneto-Active Polymers. Composites Part B: Engineering, 2021 215 (June): 108796. https://doi.org/10.1016/j.compositesb.2021.108796.

[25] Garcia-Gonzalez D, Hossain M. Microstructural modelling of hard-magnetic soft materials: Dipole–dipole interactions versus Zeeman effect. Extreme Mechanics Letters, 2021, 48, 101382. https://doi.org/10.1016/J.EML.2021.101382

[26] Haldar, K. Constitutive modeling of magneto-viscoelastic polymers, demagnetization correction, and field-induced Poynting effect, International Journal of Engineering Science, 2021, 165:103488

[27] Hemmatian M, Sedaghati R, Rakheja S. Characterization and modeling of temperature effect on the shear mode properties of magnetorheological elastomers. Smart Materials and Structures, 29(11), 2020, 115001. https://doi.org/10.1088/1361-665X/abb359.

[28] Haussener T, Momenzadeh N, von Lockette P. Particle organization versus volume fraction in magneto-active elastomer composites. Journal of Magnetism and Magnetic Materials, Volume 539, 2021, 168415, ISSN 0304-8853, https://doi.org/10.1016/j.jmmm.2021.168415.

[29] Hohlbein N, Shaaban A, Schmidt AM. Remote-controlled activation of self-healing behavior in magneto-responsive ionomeric composites. Polymer 2015;69:301–9.

[30] Hu W, Lum G, Mastrangeli M et al. Small-scale soft-bodied robot with multimodal locomotion. Nature 554, 81â€“85, 2018. https://doi.org/10.1038/nature25443.

[31] Huang X, Mohla A, Hong W, Bastawros AF, Feng X-Q. Magnetorheological brush–a soft structure with highly tuneable stiffness. Soft Matter 2014;10(10): 1537–43.

[32] Janbaz M, Googarchin HS. Experimental and numerical analysis on magneto-hyper-viscoelastic constitutive responses of magnetorheological elastomers: A characterization procedure, Mechanics of Materials, Volume 154, 2021, 103712, ISSN 0167-6636, https://doi.org/10.1016/j.mechmat.2020.103712.

[33] Jiao P, Chen T, Xie Y. Self-adaptive mechanical metamaterials (SMM) us- ing shape memory polymers for programmable postbuckling under thermal excitations. Compos Struct 2021;256:113053.

[34] Khanouki MA, Sedaghati R, Hemmatian M. Experimental characterization and microscale modeling of isotropic and anisotropic magnetorheological elastomers. Composites Part B: Engineering, 2019, 176:107311.

[35] Kim Y, Parada GA, Liu S, Zhao X. Ferromagnetic soft continuum robots. Science Robotics 2019; 4:33.

[36] Kim Y, Yuk H, Zhao R, Chester SA, Zhao X. Printing ferromagnetic domains for untethered fast-transforming soft materials. Nature 2018;558:7709, 274-227.

[37] Kim JG, Park JE, Won S, Jeon J, Wie JJ. Contactless manipulation of soft robots. Materials 2019;12:3065.

[38] Jeong-Hoi Koo, Alexander Dawson, Hyung-Jo Jung. Characterization of actuation properties of magnetorheological elastomers with embedded hard magnetic particles. 2012. https://doi.org/10.1177/1045389X12439635

[39] Koo JH, Khan F, Jang DD, Jung HJ. Dynamic characterization and modeling of magneto-rheological elastomers under compressive loadings. Smart Materials and Structures, 19(11), 2010. 117002. https://doi.org/10.1088/0964-1726/19/11/117002.

[40] Kramarenko, E Yu, Chertovich, A V, Stepanov, G V, Semisalova, A S, Makarova, L A, Perov, N S, Khokhlov, A R. Magnetic and viscoelastic response of elastomers with hard magnetic filler. Smart Materials and Structures. 2015.

[41] Lee H, Jang Y, Choe JK, Lee S, Song H, Lee JP, et al. 3D-printed programmable tensegrity for soft robotics. Science Robotics 2020;5:eaay9024.

[42] Lee K, Yu K, Al B, Hasan B, Xin A, Feng Z. Sharkskin-inspired magnetoactive reconfigurable acoustic metamaterials. Research 2020;2020:1–13.

[43] Lei Y, Sheng Z, Zhang J, et al. Building magnetoresponsive composite elastomers for bionic locomotion applications. J Bionic Eng 2020;17:405–20

[44] Liu, M.; Zhang, M.; Zhang, J.; Qiao, Y.; Zhai, P. Experimental Investigation on the Effect of Graphene Oxide Additive on the Steady-State and Dynamic Shear Properties of PDMS-Based Magnetorheological Elastomer. Polymers 2021, 13, 1777. https://doi.org/10.3390/polym13111777

[45] Lu H, Zhang M, Yang Y, et al. A bioinspired multilegged soft millirobot that functions functions in both dry and wet conditions. Nature Commun 2018;9:3944.

[46] Lucarini, S., Hossain, M., Garcia-Gonzalez, D. (2022). Recent advances in hard-magnetic soft composites: Synthesis, characterisation, computational modelling, and applications. Composite Structures, 279, 114800. https://doi.org/10.1016/J.COMPSTRUCT.2021.114800

[47] Lum GZ, Ye Z, Dong X, Marvi H, Erin O, Hu W, et al. Shape-programmable magnetic soft matter. Proc Natl Acad Sci 2016;113(41):E6007–15.

[48] Montgomery SM, Wu S, Kuang X, Armstrong CD, Zemelka C, Ze Q, Zhang R, Zhao R, Qi HJ. Magneto-Mechanical Metamaterials with Widely Tunable Mechanical Properties and Acoustic Bandgaps. Advanced Functional Materials, 2021. 31(3), 2005319. https://doi.org/10.1002/adfm.202005319

[49] Moreno MA, Gonzalez-Rico G, Lopez-Donaire ML, Arias A, Garcia-Gonzalez D. New experimental insights into magneto-mechanical rate dependences of magnetorheological elastomers. Composites Part B: Engineering 2021.

[50] Moreno MA, Gonzalez-Rico J, Gomez-Cruz C, Nunez-Sardinha E, Lopez-Donaire ML, Lucarini S, Arias A, Muñoz-Barrutia A, Velasco D, Garcia-Gonzalez D. Magneto-Mechanical System to Reproduce and Quantify Complex Strain Patterns in Biological Materials. Applied Materials Today 2022, 27:101437.

[51] Mukherjee, D., Rambausek, M., Danas, K. (2021). An explicit dissipative model for isotropic

hard magnetorheological elastomers. Journal of the Mechanics and Physics of Solids, 151, 104361. https://doi.org/10.1016/J.JMPS.2021.104361

[52] Najgebauer M, Szczyglowski J, Slusarek B, Przybylski M, Kaplon A, Rolek J. Magnetic composites in electric motors. In: Analysis and simulation of electrical and computer systems. Lecture notes in electrical engineering, vol. 452, Springer; 2018.

[53] Novelino LS, Ze Q, Wu S, Paulino GH, Zhao R. Untethered control of functional origami microrobots with distributed actuation. Proc Natl Acad Sci 2020;117(39):24096–101.

[54] Pelteret JP, Steinmann P. Magneto-Active Polymers: Fabrication, Characterisation, Modelling and Simulation at the Micro- and Macro-Scale. De Gruyter 2020. https://doi.org/10.1515/9783110418576.

[55] Qiji Ze, Xiao Kuang, Shuai Wu, Janet Wong, S Macrae Montgomery, Rundong Zhang, Joshua M Kovitz, Fengyuan Yang, H Jerry Qi, Ruike Zhao. Magnetic Shape Memory Polymers with Integrated Multifunctional Shape Manipulation. Advanced Materials. 2019. https://doi.org/10.1002/adma.201906657

[56] Ren Z, Hu W, Dong X, Sitti M. Multi-functional soft-bodied jellyfish-like swimming, Nature Communications 2019, 10:2703.

[57] Sheridan, R, Roche, J, Lofland, S, and von Lockette, P. Numerical Simulation and experimental validation of the large deformation bending and folding behavior of magnetoactive elastomer composites. Smart Mater. Struct., 2014, 23:094004-094004-14.

[58] Song H, Lee H, Lee J, Choe JK, Lee S, Yi JY, et al. Reprogrammable ferromagnetic domains for reconfigurable soft magnetic actuators. Nano Lett 2020;20:5185–92.

[59] Sorokin VV, Stepanov GV, Vasiliev VG, Kramarenko EY, Mayer M, Shamonin M, Monkman GJ. Investigation of Dynamic Modulus and Normal Force of Magnetorheological Elastomers with Soft and Hard Magnetic Fillers - NANO 2014 Schedule, Section 06 – Polymer, Organic and Other Soft Matter Materials. Moscow 14. July 2014.

[60] Stepanov GV, Chertovich AV, Kramarenko EY. Magnetorheological and deformation properties of magnetically controlled elastomers with hard magnetic filler. Journal of Magnetism and Magnetic Materials, 2012. 324:21:3448-3451

[61] Stepanov GV, Kramarenko EY, Semerenko DA. Magnetodeformational effect of the magnetoactiveelastomer and its possible applications - 2013 J. Phys.: Conf. Ser.412 012031. doi:10.1088/1742-6596/412/1/012031

[62] G.V.Stepanov, D.Yu., BorinA.V., BakhtiiarovP.A.Storozhenko. Negative coercivity of magnetic elastomers filled with magnetically hard particles. Journal of Magnetism and Magnetic Materials. 2020.

[63] Stepanov, GV, Borin, DY, Bakhtiiarov, AV, Storozhenko, PA. Influence of the size of magnetic filler particles on the properties of hybrid magnetic elastomer with magnetically hard filler. Journal of Magnetism and Magnetic Materials. 2020.

[64] Stepanov GV, Borin DY, Bakhtiiarov AV, Storozhenko PA. Hybrid magnetic elastomers prepared on the basis of a SIEL-grade resin and their magnetic and rheological properties. 2020.

[65] Stepanov, GV, Borin, DY, Kramarenko, EY, Bogdanov, VV, Semerenko, DA, Storozhenko, PA. Magnetoactive elastomer based on magnetically hard filler: Synthesis and study of viscoelastic and damping properties. Polymer Science Series A. 2014.

[66] Stepanov, GV, Borin, DY, Storozhenko, PA. Rotation of magnetic particles inside the polymer matrix of magnetoactive elastomers with a hard magnetic filler. Journal of Magnetism and Magnetic Materials, 2017, 431, 138â€“140. https://doi.org/10.1016/J.JMMM.2016.07.051

[67] Stepanov GV, Borin DY, Bakhtiiarov AV, Lobanov DA, Storozhenko PA. Ring-like structures in magnetoactive elastomers based on magnetic hard powder. Smart Materials and Structures, 2021, 30:015023

[68] Sun C, Gao Y, Wang B, Cao X, Xuan S, Gong X. Unconventional deformation and sound absorption properties of anisotropic magnetorheological elastomers. Smart Mater. Struct. 2021, 30 105022

[69] Swaroop KV, Aruna MN, Kumar H, Rahman MR. Investigation of steady state rheological properties and sedimentation of coated and pure carbonyl iron particles based magneto-rheological fluids, Materials Today: Proceedings, Volume 39, Part 4, 2021, Pages 1450-1455, ISSN 2214-7853, https://doi.org/10.1016/j.matpr.2020.05.364.

[70] Tajeddini V, Muliana A. Deformations of flexible and foldable electro-active composite structures. Compos Struct 2017;160:280â€“91.

[71] Nam TH, Petrikova I, Marvalova B. Experimental characterization and viscoelastic modeling of isotropic and anisotropic magnetorheological elastomers. Polymer Testing. Volume 81. 2020. 106272. ISSN 0142-9418. https://doi.org/10.1016/j.polymertesting.2019.106272.

[72] Vaganov MV, Borin DY, Odenbach S, Raikher YL. Training effect in magnetoactive elastomers due to undermagnetization of magnetically hard filler. Physica B: Condensed Matter, 2020, 578, 411866. https://doi.org/10.1016/J.PHYSB.2019.411866

[73] Wallin TJ, Pikul J, Shepherd RF. 3D printing of soft robotic systems. Nature Reviews Materials 2018;3:84–100.

[74] Walter BL, Pelteret JP, Kaschta J, Schubert DW, Steinmann P. On the wall slip phenomenon of elastomers in oscillatory shear measurements using parallel-plate rotational rheometry: I. Detecting wall slip. Polymer Testing, 2017, https://doi.org/10.1016/j.polymertesting.2017.05.035

[75] Walter BL, Pelteret JP, Kaschta J, Schubert DW, Steinmann P. Preparation of magnetorheological elastomers and their slip-free characterization by means of parallel-plate rotational rheometry. Smart Materials and Structures, 2017, 10.1088/1361-665X/aa6b63

[76] Wang L, Zheng D, Harker P, Patel AB, Guo CF, Zhao X. Evolutionary design of magnetic soft continuum robots. Proc Natl Acad Sci 2021;118(21):e2021922118.

[77] Wang L, Kim Y, Guo GF, Zhao X. Hard-magnetic elastica. J Mech Phys Solids 2020, 142:104045.

[78] Wu H, Xu Z, Wang J, Bo X, Tang Z, Jiang S, Zhang G. Chain formation mechanism of magnetic particles in magnetorheological elastomers during pre-structure. Journal of Magnetism and Magnetic Materials, 2021, 527: 167693. 10.1016/J.JMMM.2020.167693

[79] Wu S, Hu W, Ze Q, Sitti M, Zhao R. Multifunctional magnetic soft composites: A review. Multifunctional Mater 2020;3:042003.

[80] Xu C, Yang Z, Lum GZ. Small-scale magnetic actuators with optimal six degrees-of-freedom. Adv Mater 2021;2100170 Diller E, Sitti M. Three-dimensional programmable assembly by untethered magnetic robotic micro-grippers. Adv Funct Mater 2014;24:4397–404.

[81] Yu K, Xin A, Wang Q. Mechanics of light-activated self-healing polymer networks. J Mech Phys Solids 2019;124:643â€“62.

[82] Zare M, Prabhakaran MP, Parvin N, Ramakrishna S. Thermally-induced two-way shape memory polymers: Mechanisms, structures, and applications. Chem Eng J 2019;374:706â€“20.

[83] Ze Q, Kuang X, Wu S, Wong J, Montgomery SM, Zhang R, et al. Magnetic shape memory polymers with integrated multifunctional shape manipulation. Adv Mater 2019;32:1906657.

[84] Guang Zhang, Huixing Wang, Jiong Wang, Jiajia Zheng, Qing Ouyang, The impact of CIP content on the field-dependent dynamic viscoelastic properties of MR gels, Colloids and Surfaces A: Physicochemical and Engineering Aspects, Volume 580, 2019, 123596, ISSN 0927-7757, https://doi.org/10.1016/j.colsurfa.2019.123596.

[85] Zhang C, Li J, Yang C, Gong S, Jiang H, Sun M, et al. A pH-sensitive coordination polymer network-based nanoplatform for magnetic resonance imaging-guided cancer chemo-photothermal synergistic therapy. Nanomedicine: Nanotechnology Biol Med 2020;23:102071.

[86] Zhang J, Guo Y, Hu W, Soon RH, Davidson ZS, Sitti M. Liquid crystal elastomer-based magnetic composite films for reconfigurable shape-morphing soft miniature machines. Adv Mater 2021;33:2006191.

[87] Xu T, Zhang J, Salehizadeh M, Onaizah O, Diller E. Millimeter-scale flexible robots with programmable three-dimensional magnetization and motions. Science Robotics 2019;4(29):eaav4494.

[88] Zhao R, Kim Y, Chester SA, Sharma P, Zhao X. Mechanics of hard-magnetic soft materials, Journal of the Mechanics and Physics of Solids, Volume 124, 2019, Pages 244-263, ISSN 0022-5096, https://doi.org/10.1016/j.jmps.2018.10.008.